Single-wire photodetectors based on InGaN/GaN radial quantum wells in GaN wires grown by catalyst-free metal-organic vapor phase epitaxy

A. De Luna Bugallo,[1] L. Rigutti,[1,a] G. Jacopin,[1] F. H. Julien,[1] C. Durand,[2] X. J. Chen,[2] D. Salomon,[2] J. Eymery,[2] and M. Tchernycheva[1]

[1] *Institut d'Electronique Fondamentale, UMR CNRS 8622, Université Paris Sud 11, 91405 Orsay Cedex, France*

[2] *Equipe mixte "Nanophysique et semiconducteurs," CEA/CNRS/Université Joseph Fourier, CEA, INAC, SP2M, 17 rue des Martyrs, 38054 Grenoble Cedex 9, France*

(Received 21 February 2011; accepted 6 May 2011; published online 8 June 2011)

We present a letter on single-wire photodetectors based on radial *n-i-n* multiquantum well (QW) junctions. The devices are realized from GaN wires grown by catalyst-free metalorganic vapor phase epitaxy coated at their top by five nonpolar $In_{0.16}Ga_{0.84}N/GaN$ undoped radial QWs, and are sensitive to light with energy $E>2.6$ eV. Their photoconductive gain is as high as 2×10^3. The scanning photocurrent microscopy maps evidence that the detector response is localized at the extremity containing the QWs for both below (at $\lambda=488$ nm) and above GaN band gap (at $\lambda=244$ nm) excitation. This confirms that the device operates as a radial *n-i-n* junction. © *2011 American Institute of Physics*. [doi:10.1063/1.3596446]

In the last decade, nanowire (NW) based photodetectors have attracted much attention because of their high sensitivity.[1–6] In the III-N materials system, highly sensitive photodetectors based on binary GaN NWs (Refs. 7–9) and on polar axial GaN/AlN heterostructured NWs (Ref. 10) have been demonstrated. Radial polar and semipolar InGaN/GaN multiquantum well (MQW) NWs have already proved their potential for light emission[11,12] and photovoltaic applications.[13] In this letter, we present a study of single-wire photodetectors based on nonpolar radial InGaN/GaN MQWs. Nominally undoped MQWs sandwiched between unintentionally doped GaN core and n-doped shell layers are grown at the top of a n-doped GaN wire by catalyst-free metal-organic vapor phase epitaxy (MOVPE). These detectors respond to visible and UV light with energy above 2.6 eV. The scanning photocurrent (PC) microscopy maps demonstrate that the photoresponse is localized in the MQW region of the wire. A responsivity as high as 8.3×10^3 A/W and a −3 dB frequency cutoff of 50 Hz is measured for the device under 5 V bias illuminated with 360 nm light. We demonstrate thus that the catalyst-free MOVPE allows for the fabrication of sensitive nanoscale detectors, whose spectral properties can be tuned in the visible-near UV interval through the band engineering of the nonpolar MQW system. These systems also represent a step toward the demonstration of radial nonpolar *p-i-n* structures which could be simultaneously operated as light emitters in forward bias and photodetectors in reverse bias.[14]

The *c*-oriented GaN wires are grown by MOVPE on *c*-sapphire substrates using *in situ* SiN_x thin film predeposition.[15,16] The stem of the wires is grown at 1000 °C using trimethylgallium and ammonia with a silane addition to get n^+-doping. The silane flux is then switched off to grow unintentionally doped GaN at the top of the wires. Finally, GaN wires are coated at their top with five unintentionally doped radial InGaN/GaN quantum wells, which grow on the nonpolar m-plane facets [see the scanning electron microscopy (SEM) image of Fig. 1(a) and the schematic in Fig. 1(b)]. The covering of the top c-plane facet of the wire will be neglected due to the c- to m-plane surface area ratio. InGaN wells and GaN barriers are grown at 730 °C and 840 °C, respectively, using trimethylindium and triethylgallium as III-precursor sources. The last GaN quantum barrier is n-doped with silane to form an *n-i-n* junction. The In concentration in the QWs estimated by time-of-flight

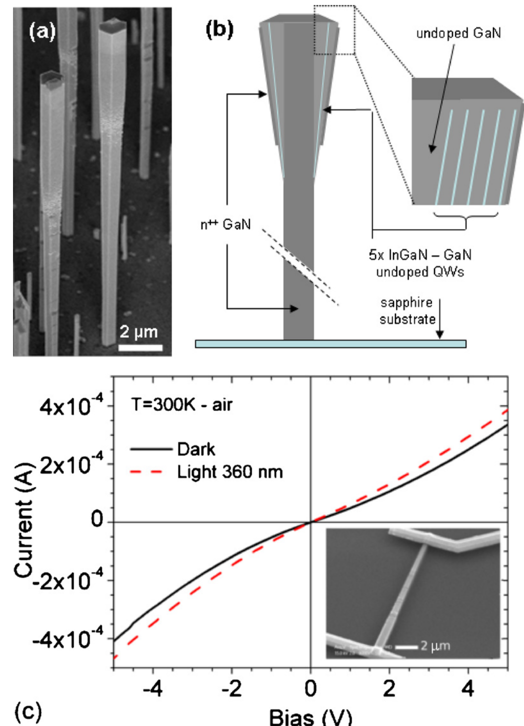

FIG. 1. (Color online) (a) SEM image of the as-grown NWs on sapphire substrate; (b) scheme of the heterostructure and of the doping profile; (c) *I-V* curves of a single-nanowire device (W1) at RT in air, in the dark (black solid line), and under illumination at $\lambda=360$ nm and $P_{inc}=30$ mW/cm^2 (red dashed line). In the inset, SEM image of the corresponding device. The NW length is 20 μm.

[a] Author to whom correspondence should be addressed. Electronic mail: lorenzo.rigutti@ief.u-psud.fr.

 © 2011 American Institute of Physics

Author complimentary copy. Redistribution subject to AIP license or copyright, see http://apl.aip.org/apl/copyright.jsp

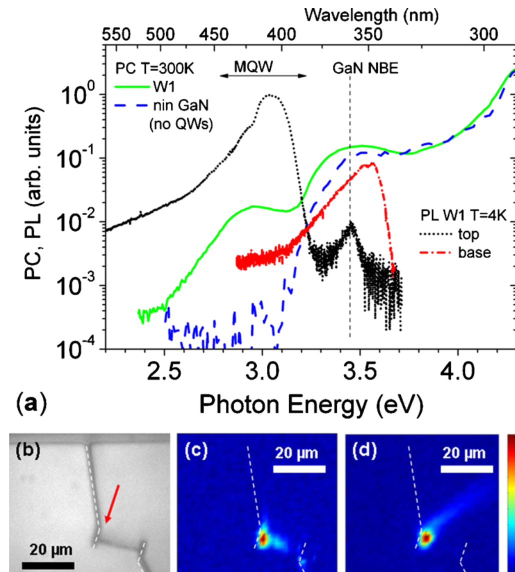

FIG. 2. (Color online) (a) Normalized PC spectrum of W1 at 1 V bias (green solid line) and of a nanowire from a reference *n-i-n* GaN sample without QWs (blue dashed line); μ-PL spectra from the top (black dotted line); and from the base (red dash-dotted line) of W1; all spectra have been collected at RT in air. (b) UV micrograph visualizing the area containing the contacted W1 analyzed by means of SPCM. The red arrow points to the NW top. [(c) and (d)] SPCM images collected exciting the sample with laser light at (c) $\lambda = 488$ nm and (d) $\lambda = 244$ nm. The scale reported on the right-hand side is linear from 0 to the maximum PC recorded within each image.

secondary ion mass spectrometry is about 16% ($\pm 4\%$) and the QW (barrier) thicknesses have been estimated from transmission electron microscopy measurements to be $t_{QW} = 1$ nm ($t_{barr} = 10$ nm). The wires selected for device processing have a length l_W (diameter d_W) in the 15–20 μm (500 nm–1 μm) range. The wire RT photoluminescence shows an intense emission at 3.05 eV attributed to the luminescence of InGaN QWs in the quantum confinement regime, below the 3.51 eV n-doped GaN band gap [Fig. 2(b)].

In order to fabricate single-wire photodetectors, wires were detached from the growth substrate by sonication in ethanol, and then dispersed on a patterned Si/SiO_2 substrate. Subsequently, they were planarized by spin coating with a layer of H-Silsesquioxane (HSQ) spin-on glass with thickness $t_{HSQ} \sim 500$ nm and then annealed at 700 °C for 30 min in order to transform the HSQ into SiO_x. This layer is required to provide a solid support for continuous metallic contacts. Dry etching using CF_4 chemistry was then performed to uncover the upper side of the NWs from residual SiO_x. The contacts to the NW extremities have been fabricated by e-beam lithography and Ti/Al/Ti/Au metallization. It is important to note that during the growth the QWs are formed only at the NW top. This allows contacting directly the wire core without intermediate etching steps, as it has been done in analogous core-shell NW devices.[11] The SEM image of a planarized and contacted wire is reported in the inset of Fig. 1(c). A total of ten objects have been processed and subsequently studied, yielding a good reproducibility. In the following, we will refer to the measurements performed on one particular device, labeled W1, if not otherwise specified.

The wire current-voltage (*I-V*) characteristics were tested using a probe station and a Keithley 2636 sourcemeter. The *I-V* curves of W1 are reported in Fig. 1(c), measured at RT in ambient air under different illumination conditions. The curves are symmetric and quasi-ohmic, with a dark resistance at zero-bias $R_0 = 20$ kΩ. No change in the *I-V* characteristics occurs under vacuum or when illuminating with light at $\lambda > 520$ nm.

Upon illumination at a wavelength $\lambda = 360$ nm with incident power density $P_{inc} = 30$ mW/cm^2, the conductivity of the NW device increases, yielding a PC $I_{PC} = 5 \times 10^{-5}$ A under 5 V bias. Taking into account the wire exposed area where the lateral overgrowth occurred, this corresponds to a responsivity $\mathfrak{R}(360$ nm$, 5$ V$) = 2.5 \times 10^4$ A/W. As the device is an *n-i-n* junction, the PC is generated through a photoconductive mechanism, with the production of excess carriers within the undoped region.[17] The photoconductive gain, defined as the ratio between collected photogenerated carriers and absorbed photons per unit time—assuming that all incident photons are absorbed—is $G(360$ nm$, 5$ V$) = 9.2 \times 10^3$. For illumination under band gap at $\lambda = 400$ nm, we obtain a responsivity $\mathfrak{R}(400$ nm$, 5$ V$) = 1.6 \times 10^4$ A/W and a gain $G(400$ nm$, 5$ V$) = 5.2 \times 10^3$. This gain value $G \gg 1$ suggests that a spatial separation mechanism strongly suppresses the recombination of the photogenerated e-h pairs.[1,5,7,8] Such an effect has been previously reported in smaller diameter axial NW photodetectors because of the localization of holes (electrons) at the periphery (center) of the NW due to radial band bending.[1,2,7,8] In these radial junctions the carrier separation mechanism must be different. This mechanism is most likely related to the presence of an upward band bending along the NW axis. The resulting electric field attracts the photogenerated holes toward the top polar surface, and separates them from electrons in the active region, as previously reported in the case of bulk GaN-based *n-i-n* photoconductors.[18] Moreover, holes may be trapped at the top surface yielding a diminution of the surface space charge region, contributing thus to the increase in the device conductivity.[18]

The NW PC spectra were measured using a tunable visible-UV light source, consisting of a Xe lamp coupled with a Jobin Yvon Triax 180 spectrometer. The spectral resolution of the system used in this letter is ~40 meV. The PC spectrum of W1 recorded at RT in air and under bias $V_b = 1$ V is shown in Fig. 2(a), normalized by the incident power of the monochromatized light. The onset of the PC is at $E = 2.5$ eV. A significant PC contribution is therefore found below the GaN band gap. The spectrum exhibits a second PC onset at $E \sim 3.3$ eV, close to the GaN near-band edge (NBE) energy, then the signal extends to the deep UV range. We notice that the PC spectrum of a *n-i-n* GaN reference wire without QWs does not exhibit any subband gap signal comparable to that of W1. The PC spectrum of W1 can also be compared to its microphotoluminescence (μ-PL) spectrum acquired at $T = 4$ K exciting the top of the wire with 244 nm laser light [Fig. 2(a)]. This spectrum exhibits two main peaks: (i) a broad peak at $E_{QW} = 3$ eV, corresponding to the emission of the MQWs and (ii) a second peak at $E_{NBE} = 3.45$ eV, at the GaN NBE. The μ-PL from the base of the same wire [Fig. 2(a)] only exhibits the GaN NBE peak, blueshifted at $E_{NBE} = 3.56$ eV because of the high doping concentration ($N_d \sim 10^{20}$ cm^{-3}).[15] We attribute therefore the sub-bandgap PC to transitions taking place within the radial MQW system. The PC onset at $E = 3.3$ eV is most likely related to photogeneration in the unintentionally doped GaN barriers in the MQW region. A slight redshift with respect to the GaN band gap can be explained by band tailing

Author complimentary copy. Redistribution subject to AIP license or copyright, see http://apl.aip.org/apl/copyright.jsp

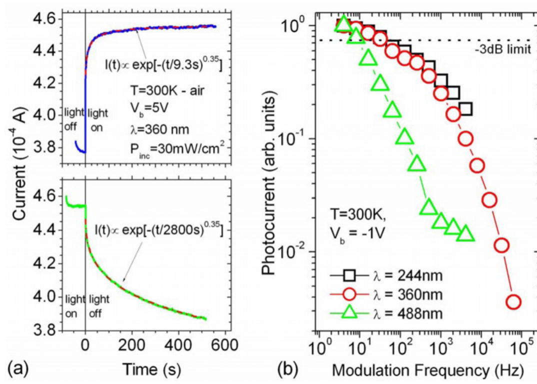

FIG. 3. (Color online) (a) Time response of W1 polarized at V_b=5 V to light steps. (b) Normalized frequency response of the detector to modulated light at λ=244 nm (black squares), at λ=360 nm (red circles) and at λ=488 nm (green triangles).

effects. Within the measurement range of the techniques employed, no yellow band or other defect-related signal could be found.

We investigated the spatial distribution of PC generation by means of spatial PC microscopy (SPCM),[19] also known as optical beam-induced current.[20] The sample was illuminated with laser light either at λ=488 nm or at λ=244 nm focused by 20x objective lens with 0.4 numerical aperture. The PC map was obtained by scanning the sample by means of an automated X-Y piezoelectric stage. The spatial resolution was about 2 μm. The optical microscopy picture of the analyzed area containing W1 is visualized in Fig. 2(b) while the two SPCM images are reported in Figs. 2(c) and 2(d). For both excitation wavelengths the PC signal is located exclusively in the immediate neighborhood of the NW top, in correspondence with the unintentionally doped MQW region. The PC signal along the NW body is very low, confirming that the PC is generated in the intrinsic region even for an excitation above the GaN band gap as expected for a radial *n-i-n* junction. The overall device conductivity increases indeed only when the resistivity of the undoped portion drops because of the generation of free electron-hole pairs.

Figure 3(a) displays the rise and decay current transients of the device under illumination at λ=360 nm. In both transients we can identify a fast and a persistent component. This latter was identified by fitting both transients by a stretched exponential $I(t)=I_0+A\ \exp[-(t/\tau)^{\alpha}]$ with $\alpha=0.35$. The time constant τ is ~10 s for the rising time and of the order of 3000 s for the decay time. These results are in good agreement with the persistent PC studies reported in the case of bulk GaN UV photodetectors[21,22] and GaN NW detectors.[9] To identify the fast component, the response to modulated light was monitored at three different wavelengths (λ=244, 360, and 488 nm). The results, illustrated in Fig. 3(b), show that for the two UV wavelengths the −3 dB cutoff[23] is at f_T~50 Hz, corresponding to the fast component characteristic time τ~3 ms. The cutoff drops to f_T~20 Hz for light at λ=488 nm. The observed persistent PC behavior can be explained keeping into account the spatial separation of carriers and the modulation of the surface space charge width by hole trapping.[18] However, the difference in the cutoff frequency for UV and visible light indicates that the hole trapping mechanism may be different in the case of GaN and QW excitation, respectively.

In conclusion, we have demonstrated that high sensitivity photodetectors can be fabricated using radial InGaN/GaN MQW *n-i-n* junctions in single wires grown by catalyst-free MOVPE. The devices exhibit a high responsivity (~8 $\times 10^3$ A/W) in the visible-to-UV spectral range and a frequency response with a −3 dB cutoff of 50 Hz. This study demonstrates the interest of the radial InGaN QWs for the development of NW optoelectronic devices such as photodetectors and light-emitting diodes.

This work was supported by the French ANR Agency under the Programs Nos. ANR-08-NANO-031 BoNaFO and ANR-08-BLAN-0179 NanoPhotoNit. The authors also acknowledge J. C. Barnes for SIMS measurements. A.D.L.B. acknowledges the Mexican National Council on Science and Technology (CONACYT) for PhD Scholarship No. 210683.

[1]C. Soci, A. Zhang, B. Xiang, S. A. Dayeh, D. P. R. Aplin, J. Park, X. Y. Bao, Y. H. Lo, and D. Wang, Nano Lett. **7**, 1003 (2007).
[2]C. Soci, A. Zhang, X. Y. Bao, H. Kim, Y. Lo, and D. Wang, J. Nanosci. Nanotechnol. **10**, 1430 (2010).
[3]H. Kind, H. Yan, B. Messer, M. Law, and P. Yang, Adv. Mater. (Weinheim, Ger.) **14**, 158 (2002).
[4]X. Fang, T. Zhai, U. K. Gautam, L. Li, L. Wu, Y. Bando, and D. Golberg, Prog. Mater. Sci. **56**, 175 (2011).
[5]G. Konstantatos and E. H. Sargent, Nat. Nanotechnol. **5**, 391 (2010).
[6]L. VJ, J. Oh, A. P. Nayak, A. M. Katwenmeyer, K. H. Gilchrist, S. Grego, N. P. Kobayashi, S. Y. Wang, A. A. Talin, N. K. Dhar, and M. S. Islam, “A perspective on nanowire photodetectors: Current status, future challenges, and opportunities,” IEEE J. Sel. Top. Quantum Electron (to be published).
[7]R. Calarco, M. Marso, T. Richter, A. I. Aykanat, R. Meijers, A. d. Hart, T. Stoica, and H. Lüth, Nano Lett. **5**, 981 (2005).
[8]R. S. Chen, H. Y. Chen, C. Y. Lu, K. H. Chen, C. P. Chen, L. C. Chen, and Y. J. Yang, Appl. Phys. Lett. **91**, 223106 (2007).
[9]N. A. Sanford, P. T. Blanchard, K. A. Bertness, L. Mansfield, J. B. Schlager, A. W. Sanders, A. Roshko, B. B. Burton, and S. M. George, J. Appl. Phys. **107**, 034318 (2010).
[10]L. Rigutti, M. Tchernycheva, A. De Luna Bugallo, G. Jacopin, F. H. Julien, L. F. Zagonel, K. March, O. Stephan, M. Kociak, and R. Songmuang, Nano Lett. **10**, 2939 (2010).
[11]F. Qian, Y. Li, S. Gradecak, D. Wang, C. J. Barrelet, and C. M. Lieber, Nano Lett. **4**, 1975 (2004).
[12]F. Qian, Y. Li, S. Gradecak, H. G. Park, Y. J. Dong, Y. Ding, Z. L. Wang, and C. M. Lieber, Nature Mater. **7**, 701 (2008).
[13]Y. Dong, B. Tian, T. J. Kempa, and C. M. Lieber, Nano Lett. **9**, 2183 (2009).
[14]Q. Wang, S. Savage, S. Persson, B. Noharet, S. Junique, J. Y. Andersson, V. Liuolia, and S. Marcinkievičius, Proc. SPIE **7216**, 721627 (2009).
[15]R. Koester, J. S. Hwang, C. Durand D. Le Si Dang, and J. Eymery, Nanotechnology **21**, 015602 (2010).
[16]X. J. Chen, G. Perillat-Merceroz, D. Sam-Giao, C. Durand, and J. Eymery, Appl. Phys. Lett. **97**, 151909 (2010).
[17]E. Monroy, F. Omnès, and F. Calle, Semicond. Sci. Technol. **18**, R33 (2003).
[18]J. A. Garrido, E. Monroy, E. Izpura, and E. Muñoz, Semicond. Sci. Technol. **13**, 563 (1998).
[19]Y. Gu, J. P. Romankiewicz, J. K. Davis, J. L. Lensch, L. J. Lauhon, E. S. Kwak, and T. W. Odom, J. Vac. Sci. Technol. B **24**, 2172 (2006).
[20]T. Wilson and E. M. McCabe, J. Appl. Phys. **61**, 191 (1987).
[21]H. M. Chen, Y. F. Chen, M. C. Lee, and M. S. Feng, J. Appl. Phys. **82**, 899 (1997).
[22]O. Katz, G. Bahir, and J. Salzman, Appl. Phys. Lett. **84**, 4092 (2004).
[23]As the present device does not follow the behavior of a linear filter, the –3 dB cutoff f_T is here defined according to the relationship $20\log[I(f_T)/I(f_0=4\ \text{Hz})]=-3$, where I is the PC signal.

Author complimentary copy. Redistribution subject to AIP license or copyright, see http://apl.aip.org/apl/copyright.jsp